PCCP

Cite this: *Phys. Chem. Chem. Phys.*, 2012, **14**, 11363–11370

www.rsc.org/pccp

PAPER

Performance of the M11 and M11-L density functionals for calculations of electronic excitation energies by adiabatic time-dependent density functional theory

Roberto Peverati and Donald G. Truhlar*

Received 23rd April 2012, Accepted 28th May 2012
DOI: 10.1039/c2cp41295k

Adiabatic time-dependent density functional theory is a powerful method for calculating electronic excitation energies of complex systems, but the quality of the results depends on the choice of approximate density functional. In this article we test two promising new density functionals, M11 and M11-L, against databases of 214 diverse electronic excitation energies, and we compare the results to those for 16 other density functionals of various kinds and to time-dependent Hartree–Fock. Charge transfer excitations are well known to be the hardest challenge for TDDFT. M11 is a long-range-corrected hybrid meta-GGA, and it shows better performance for charge transfer excitations than any of the other functionals except M06-HF, which is a specialized functional that does not do well for valence excitations. Several other long-range-corrected hybrid functionals also do well, and we especially recommend M11, ωB97X, and M06-2X for general spectroscopic applications because they do exceptionally well on ground-state properties as well as excitation energies. Local functionals are preferred for many applications to extended systems because of their significant cost advantage for large systems. M11-L is a dual-range local functional and—unlike all previous local functionals—it has good performance for Rydberg states as well as for valence states. Thus it is highly recommended for excitation energy calculations on extended systems.

1 Introduction

Electronic excitations of molecules may be roughly divided into three classes: (i) local valence excitations in which the principal quantum number does not change and there is no site-to-site shift of electron density, except perhaps to neighbouring sites, (ii) Rydberg transitions in which the atomic or united-atom principal quantum number increases, and (iii) charge transfer excitations involving a charge shift between different atoms.

The ability of time-dependent density functional theory[1–4] (TDDFT) to calculate such excitation energies by using the adiabatic approximation and conventional exchange–correlation functional approximations (for brevity simply called functionals in the remainder of the article) has been investigated thoroughly, but further comparisons are useful whenever new and improved functionals for ground states are introduced. In general, functionals that are developed for ground-state properties provide different levels of accuracy for the three prototype classes of excitations. For example, a recent article[5] concluded that "No functional ... shows acceptable accuracy for all three of valence, Rydberg, and charge transfer excitations". Recent developments in density functional approximations, and new investigations of excitation energies using TDDFT, show promising results for some difficult excitation energies,[6–13] as well as notable improvements for ground-state properties.[11,14] A central issue in understanding performance has been distinguishing between hybrid functionals, which combine nonlocal Hartree–Fock exchange with local density functional exchange (where "local" includes dependence on any local electronic variable, including spin-labelled densities, their reduced gradients, and spin-labelled orbital-dependent kinetic energy densities), and local functionals, which have only the latter. Local functionals tend to be inaccurate for Rydberg excitations and are always inaccurate for charge-transfer excitations, although they are widely used because they are more computationally affordable for extended systems. A key development was the introduction of so-called long-range-corrected functionals,[15,16] which are fully nonlocal in the asymptotic limit of long-range electron–electron interactions and local or hybrid for finite-range (*i.e.*, short-range) interactions. The long-range-corrected formalism is more flexible than the older strategy of global hybrids, which have a fixed percentage of nonlocal exchange for all ranges of interelectronic separation,

Department of Chemistry and Supercomputing Institute, University of Minnesota, Minneapolis, MN 55455-0431, USA. E-mail: truhlar@umn.edu

and it is capable of higher accuracy. Both long-range corrected functionals and global hybrids are more accurate than local functionals for many ground-state properties, at least for systems that do not have high multireference character. Long-range-corrected functionals also ameliorate some of the problems of charge-transfer excitations with TDDFT, without deteriorating performance for the remaining classes of excitations and for ground-state properties,[6,11,14,17–20] but they do not lower the cost for extended systems. Long-range-corrected functionals are special cases of the more general class of functionals (discussed below) that involve range separation in various ways.

We recently proposed two new functionals, one of which, called M11-L,[14] is local, and the other of which, called M11,[11] is long-range corrected; both functionals have broad applicability in chemistry and chemical physics. They employ two different approaches to range-separation: the M11-L functional uses dual-range (DR) exchange in which both short-range and long-range exchange are treated by local functionals, and the range separation is at the local level only, while the M11 functional uses conventional range-separation, with 42.8% of Hartree–Fock (HF) exchange at short range, and 100% at long range. In this paper we address the performance of these two new functionals for calculations of excitation energies with adiabatic time-dependent density functional theory (TDDFT), and we compare them to other popular functionals.

2 Methods

2.1 Time-dependent density functional theory

Time-dependent density functional theory is a very appealing method for the calculation of excitation energies of molecules. Probably the most important reason for its success is that it includes dynamical correlation effects at a smaller computational cost than post-Hartree–Fock wave function methods. In practical calculations for chemistry, TDDFT is almost always carried out in the adiabatic approximation, using a frequency-independent approximation to the exchange–correlation functional. As we noted above, the functionals used are usually ones developed for ground states.[17,21,22]

In general, there is no unique answer to the question of which functional performs best for all three prototype classes of excitation, and if we include ground-state properties in the evaluation, the situation is even less clear. For example functionals that are very successful for a large number of ground-state properties, such as M06 and M06-2X,[22] give accurate results for local valence excitations and for low Rydberg states, but not for the more challenging charge transfer excitations, in particular those with small spatial overlap[23] of the moduli of the initial and final orbitals.[22] The M06-HF functional,[24] is very accurate for spatially nonoverlapping charge transfer (the most challenging kind), but at the price of worse accuracy for local valence states, low Rydberg states,[22] and, most importantly, many ground-state properties.[11,14]

Considering the issue of improving charge-transfer excitations while retaining good across-the-board performance, the new class of range-separated functionals seems to at least partially solve the problems of local and global hybrid functionals for such excitations. In the present article we investigate this problem further by testing the performance of two recently developed range-separated functionals for TDDFT excitation energies calculations of all three types of excitations. The results presented in this article are complimentary to those of other validation studies published recently.[5,7,13,20,25–28]

The new functionals are briefly described in the following subsection, but the reader is referred to the original articles[11,14] for full details.

2.2 Range-separation and the 2011 Minnesota functionals

The basic idea of range–separated functionals is that the modelling of the exchange–correlation functional can benefit from a different treatment of the Coulomb operator in the short-range (SR) and long-range (LR); therefore the operator is split:

$$\frac{1}{r_{12}} = \underbrace{\frac{\mathrm{erfc}(\omega r_{12})}{r_{12}}}_{\mathrm{SR}} + \underbrace{\frac{\mathrm{erf}(\omega r_{12})}{r_{12}}}_{\mathrm{LR}}. \qquad (1)$$

where ω is a parameter, and r_{12} is an interelectronic distance. Long-range-corrected range-separated hybrid functionals use 100% of nonlocal exchange in the LR limit to compensate part of the self–interaction error of DFT (which is possible because of the correct asymptotic behaviour of Hartree–Fock nonlocal exchange), and the amount of nonlocal exchange decreases to a value usually between 0 and 50% in the SR limit. The M11 functional that we introduced recently[11] uses this kind of range separation with the error function, with 42.8% of nonlocal exchange at the SR limit and 100% at the LR limit. A closely related range-separation strategy is that employed by the CAM-B3LYP functional,[29] which has 19% nonlocal exchange in the SR limit and 65% in the LR limit.

Another approach to range separation is to use a hybrid functional with a finite amount of nonlocal exchange at short-range, but have this tend to zero in the LR limit, which is a strategy that may be called screened exchange. The HSE functional[30] takes this approach in order to cut the computational cost of nonlocal exchange integrals for extended systems with periodic boundary conditions, while at the same time—in principle—retaining the good performance features of global hybrid functionals for most chemical properties. This kind of range-separation is also tested in the present article.

The dual-range exchange strategy of M11-L introduces yet another way to use range separation. It uses two different local functionals, one for SR and one for LR. Each local functional is a flexible meta-GGA (meta-generalized-gradient approximation), where a meta-GGA is a functional that depends on the spin-labelled densities, their reduced gradients, and the spin-labelled kinetic energy densities. The meta-GGAs are parametrized using databases of accurate reference data. The main difference between the dual-range approach (as in M11-L) and the long-range-corrected approach (as in M11) is schematically illustrated in Fig. 1. The optimized meta-GGA functional forms in M11-L are indeed different at different ranges (see, *e.g.*, Fig. 1 of ref. 14), showing that the dependence of the exchange energy density on interelectronic distance is quite different at SR and LR.

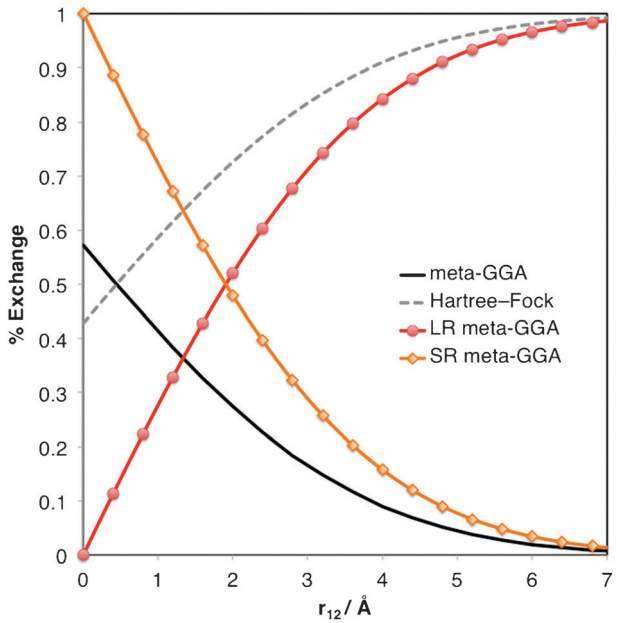

Fig. 1 Range separation in the exchange functional: The black and grey curves are for the M11 functional (local is solid, nonlocal is dashed) and the red and orange curves are M11-L (LR is red with circles, SR is orange with diamonds).

2.3 Testing the functionals

In the next section we present the databases that we used to assess the performances of the new Minnesota functionals for TDDFT excitation energies. The basis sets, the reference geometries, and the data are specified there and in the corresponding references. All calculations in this article were performed using a locally modified version[31] of *Gaussian 09*,[32] using the adiabatic TDDFT method with the ultrafine (99 radial nodes, 590 angular nodes) Lebedev grid.

3 Databases

In this work we use four main databases to evaluate the performance of the functionals. The first three databases (VES20, RES20, and CTS8) are representative of the main prototype classes of electronic excitations: valence (V), Rydberg (R), and charge-transfer (CT). The fourth database is an extensive and more diverse set of valence excitations and represents a more thorough set for assessment of functional performance. Each database is briefly introduced below, and results will be presented in the next section.

3.1 Valence excitations: the VES20 set

The VES20 database contains 20 experimental valence excited states of small molecules: N_2 (8 states), CO (7 states), HCHO (4 states), and tetracene (1 state). The augmented Sadlej pVTZ basis set[33,34] was employed for the calculations on N_2, CO, and HCHO, while the TZVP basis set was employed for tetracene.[35,36] Geometries and reference data are taken from previous work.[5,22,24] The VES20 data includes 9 singlet → singlet (S–S) transitions and 11 singlet → triplet (S–T) transitions.

3.2 Rydberg excitations: the RES20 set

The RES20 database contains experimental data for 20 Rydberg-state transitions of N_2 (5 states), CO (7 states), and HCHO (8 states), and is complementary to the VES20 set. The augmented Sadlej pVTZ basis set[33,34] was employed for all the calculations in the RES20 database on geometries taken from previous work.[5,22,24] The RES20 data includes 13 S–S transitions and 7 S–T transitions.

3.3 Charge-transfer excitations: the CTS8 set

The CTS8 database was recently introduced[11] by adding five charge–transfer excitations of bio-organic molecules to the earlier and smaller CTES3 database[24] with three charge transfer excitation energies. The CTS8 set is composed of one theoretical datum each for $NH_3\cdots F_2$ (at 6 Å), $C_2H_4\cdots C_2F_4$ (at 8 Å), and tetracene and of five singlet → singlet electronic excitation energies with varying amounts of CT for two retinals from ref. 8. The excitations in $NH_3\cdots F_2$ and $C_2H_4\cdots C_2F_4$ are characterized by almost no overlap of the initial and final orbital, while the charge transfer character of the other excitations is not so severe. Calculations for the three complexes in CTES3 are performed using the TZVP basis set, while calculations for the retinals are performed using the 6-31++G(d,p) basis set as used by Dwyer and Tozer.[37] Geometries and reference data are taken from previous work.[8,24] The CTS8 database was used previously to assess the performances of the M11 functionals, and we add here results for M11-L and other functionals. All data in CTS8 are for S–S transitions.

3.4 A larger test: the VT set

In order to base our conclusions on a very broad set of data, we use the VT database of Jacquemin *et al.*,[5] which is composed of 103 S–S and 63 S–T electronic excitations of 28 small molecules. The reference data are taken from high-level calculations (multistate complete-active-space second-order perturbation theory and coupled cluster) from Thiel and coworkers.[38–40] The name VT comes from the original work of Jacquemin *et al.*,[5] and stands for "*versus* theory"; the corresponding "*versus* experiment" (VE) set includes a large number of experimental data in solution, and needs calculation in solvated environment, for which performance might be affected by issues beyond the choice of functional. To provide an analysis of the performance of functionals that is free from possible errors in the way that solvatochromic shifts are calculated,[41] the VE set is not considered in this work. The TZVP basis set and the MP2/6-31G(d) geometry are used for the VT calculations, as in ref. 20 and 42. The basis set issue, and in particular the use of larger diffuse-function-containing basis sets, was assessed in the work of Jacquemin and coworkers.[20] We briefly checked their conclusions for the new functionals considered in this work by performing M11 calculations with the aug-cc-pVTZ basis. Our results are in line with those of Jacquemin *et al.*[20] for M06-2X and other functionals, and the variations of the main statistical data (mean signed and mean unsigned errors) by going from the smaller TZVP to the larger aug-cc-pVTZ basis are smaller than 0.02 eV, a number that is small enough to not influence the conclusions of this work.

The VT set considered here is a popular choice for benchmarking TDDFT calculations on functionals and semi-empirical methods. However, the choice of the reference data is not always undisputed. In this work we have employed the same basis set and geometries that were used by Thiel and coworkers[38–40] for MS-CASPT2 calculations, and we use their "best theoretical estimates" as our reference data. In order to clear some of the confusion, we avoid any other comparison to other estimated reference data (*e.g.* the comparison to non-converged MS-CASPT2/TZVP results that was also reported in ref. 5 is not considered here).

4 Results and discussion

In this section we present the results of TDDFT calculations with the new Minnesota functionals M11-L and M11, and we compare them to those of several other popular and high-quality functionals. The functionals included in the comparison are chosen from the extensive results published by Silva-Junior and coworkers[39] and by Jacquemin and coworkers.[5,7,20,43] We chose the functionals to compare to by considering the most popular and best performing functional for each category. For example, we chose successful local and global hybrid functionals, as well as all the functionals in the M05 and M06 families, and some of the most popular range-separated functionals. The functionals in this study are divided into the following classes:

- Local functionals (including dual-range): BLYP,[44,45] PBE,[46] M06-L,[47] and M11-L.[14]
- Global hybrid functionals: B3LYP,[44,45,48,49] PBE0,[50] M05,[51] M05-2X,[52] M06,[22] M06-2X,[22] and M06-HF.[24] These functionals have respectively 20, 25, 28, 56, 27, 54, and 100 per cent nonlocal (*i.e.*, Hartree–Fock) exchange.
- Range-separated hybrid functionals: HSE,[30] CAM-B3LYP[29] and five long-range corrected functionals: LC-ωPBE,[53] ωB97,[6] ωB97X,[6] ωB97X-D,[54] and M11.[11] Note that the first four of the long-range-corrected functionals are long-range-corrected GGAs (GGAs depend on only the spin-labelled densities and their reduced gradients), and M11 is a long-range-corrected meta-GGA.

For the VT set, we used results from the literature[5,7,20,39,43] plus our own calculations for the HSE screened exchange functional, for M11 and M11-L, and for pure Hartree–Fock (HF) theory, that is, time-dependent Hartree–Fock. For the CTS8 database, all results are our own calculations carried out for this paper. For VES20 and RES20, we carried out new calcuations for HSE, CAM-B3LYP, ωB97, ωB97X, ωB97X-D, M11, and M11-L, and we used literature results[22] for BLYP, B3LYP, PBE, PBE0, and the previous Minnesota functionals.

4.1 Prototype excitations: VES20, RES20, and CTS8

Results for the three databases of prototype excitations, valence, Rydberg, and charge-transfer, are collected in Table 1. The mean unsigned errors (MUEs) for each of the databases are reported in the table, as well as the overall mean unsigned errors for all three prototypes interactions (VRCT48), calculated as:

$$\mathrm{MUE[VRCT48]} = \{20 \times \mathrm{MUE[VES20]} + 20 \times \mathrm{MUE[RES20]} + 8 \times \mathrm{MUE[CTS8]}\}/48. \quad (2)$$

Table 1 Results (in eV) for TDDFT calculations with M11-L and M11 for three prototype transition databases: VES20, RES20 and CTS8

Functional	X^a	VES20	RES20	CTS8	VRCT48
Local functionals					
BLYP	0	0.35	2.00	2.21	1.35
PBE	0	0.32	1.95	2.87	1.42
M06-L	0	0.32	1.62	2.58	1.24
M11-L	0	0.27	0.36	1.95	0.59
Global hybrid functionals					
B3LYP	20	0.28	1.07	2.01	0.90
PBE0	25	0.29	0.86	1.84	0.79
M06	27	0.24	1.67	1.82	1.10
M05	28	0.29	1.16	1.82	0.91
M06-2X	54	0.34	0.35	1.04	0.46
M05-2X	56	0.37	0.31	1.07	0.46
M06-HF	100	0.71	0.39	0.64	0.57
HF	100	1.08	1.18	1.14	1.13
Range-separated hybrid functionals					
HSE	25–0	0.40	0.34	2.08	0.66
CAM-B3LYP	19–65	0.38	0.51	1.18	0.56
LC-ωPBE	0–100	0.36	0.15	1.20	0.41
ωB97	0–100	0.24	0.20	1.18	0.38
ωB97X	15.77–100	0.28	0.22	1.06	0.39
ωB97X-D	22.2–100	0.28	0.32	1.19	0.45
M11	42.8–100	0.34	0.30	0.98	0.43

[a] X denotes the percentage of nonlocal exchange.

Results for VES20 show generally good performance by almost all density functionals. The main trends are easily explained in terms of the percentage of HF exchange of the functional. Local functionals all perform well for this database, but are on average worse than functionals with a small percentage of HF exchange (in the range of 20 to 25%). By increasing the percentage of nonlocal exchange the MUEs tend to get worse, but they remain satisfactory even for percentages around 50%. A worsening of the results is found for 100% nonlocal exchange, as in HF itself and M06-HF, which are the worst methods for these valence excitation energies. M11-L performs slightly better than other local functionals, although not as well as the best nonlocal performers, which are M06 and ωB97. The performances of range-separated functionals are affected principally by the percentage of nonlocal exchange at SR, while the presence of 100% nonlocal exchange at LR does not worsen the results. M11 also follow the same trend, and performs about the same as those functionals with 50% nonlocal exchange.

Rydberg states constitute a large part of the higher-energy spectrum, and they often mix with valence states to a greater or lesser extent; therefore the performance of a functional for Rydberg states is particularly important for its overall evaluation. As found previously,[5] conclusions about the performance of functionals based on valence excitations can change radically when Rydberg excitations are included in the evaluation. For RES20 we find seven functionals with MUEs over 1 eV, including M06, which was the best performer for the VES20 database. The only functionals that provide satisfactory results are the long-range corrected ones and those with a high percentage of HF exchange, such as M06-HF (which is, however, worse than long-range corrected functionals). M11-L stands out from the other local functionals, with surprisingly excellent results for this set, a performance that must be explained

by the better treatment of the LR exchange made possible by the dual–range nature of the exchange.

Results for the charge-transfer database, CTS8, are also in contrast to those of the previous two databases. This set is, on average, even more problematic than the Rydberg excitations, and only M06-HF provides satisfactory results for this set. Local functionals, including M11-L, and functionals with a small percentage of HF exchange perform very badly, as expected, since they are unable to account for long-range self-interaction error, in particular when the overlap between the densities[23] is small. Global hybrids with a high percentage of nonlocal exchange and long-range corrected functionals have average errors in the range of 1 eV; M11 does the best of these, with an MUE of 0.98 eV.

In order to draw an overall conclusion about the performances of the considered functionals for prototype excitations, we calculated for each database the average MUE among all considered functionals; we find an average MUE of 0.38 eV for VES20, 0.79 eV for RES20, and 1.57 eV for CTS8. Then, again for each database, we calculated for each functional its deviation from the average MUE; these values are reported in Fig. 2 in percentage units. A functional that performs better than average for a particular database has a bar in the negative region of the plot, while a functional that

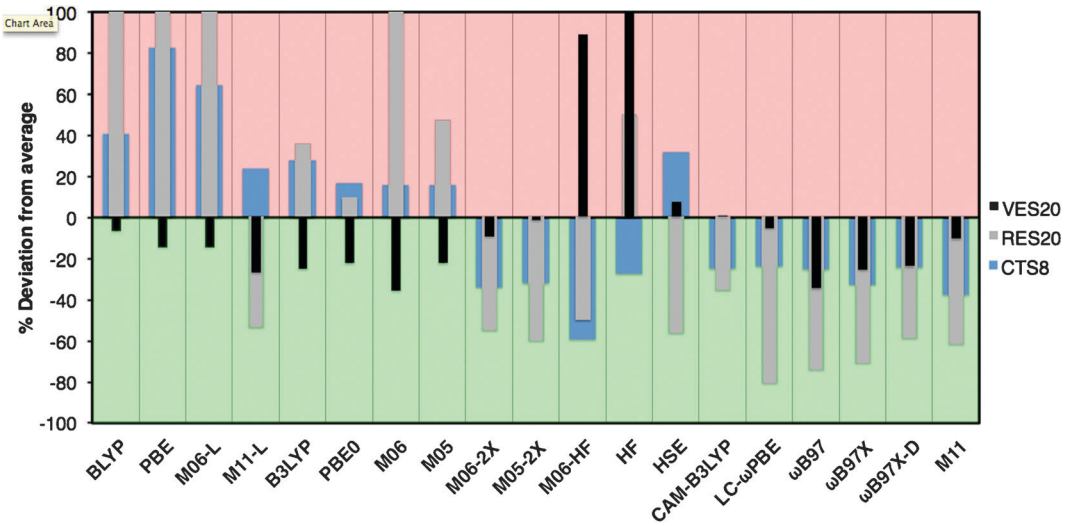

Fig. 2 Percentage deviation from the average MUE for the three databases of prototype excitations. Negative bars (in the green region) mean performance better than average, while positive bars (in the red region) mean performance worse than average. Positive errors larger than 100% are truncated to 100% for this figure.

Table 2 Results for TDDFT calculations with M11-L, M11, and 14 other functionals for the VT set[a]

		Singlets				Triplets				Total
Functional	X^b	MSE	MUE	RMSE	R^2	MSE	MUE	RMSE	R^2	MUE
Local functionals										
BLYP	0	0.47	0.54	0.63	0.92	0.48	0.49	0.58	0.93	0.52
PBE	0	0.45	0.53	0.64	0.91	0.50	0.50	0.60	0.93	0.52
M06-L	0	0.14	0.35	0.42	0.91	0.37	0.38	0.45	0.96	0.36
M11-L	0	−0.15	0.32	0.41	0.92	−0.19	0.25	0.31	0.95	0.29
Global hybrid functionals										
B3LYP	20	0.07	0.27	0.33	0.94	0.45	0.45	0.49	0.98	0.34
PBE0	25	−0.05	0.24	0.32	0.95	0.49	0.49	0.54	0.97	0.33
M06	27	0.12	0.28	0.34	0.95	0.44	0.44	0.47	0.98	0.34
M05	28	0.10	0.30	0.36	0.94	0.70	0.70	0.78	0.95	0.45
M06-2X	54	−0.23	0.34	0.46	0.92	0.07	0.23	0.28	0.94	0.30
M05-2X	56	−0.28	0.39	0.52	0.91	0.22	0.27	0.33	0.96	0.34
M06-HF	100	−0.32	0.55	0.70	0.83	−0.06	0.44	0.51	0.87	0.51
HF	100	−1.00	1.05	1.23	0.73	−1.69	1.90	2.85	0.54	1.37
Range-separated hybrid functionals										
HSE	25–0	−0.01	0.23	0.30	0.94	−0.48	0.48	0.53	0.98	0.33
CAM-B3LYP	19–65	−0.22	0.31	0.42	0.93	0.41	0.42	0.48	0.93	0.35
LC-ωPBE	0–100	−0.41	0.46	0.61	0.90	0.50	0.55	0.66	0.98	0.49
ωB97	0–100	−0.43	0.47	0.62	0.90	0.29	0.38	0.45	0.99	0.44
ωB97X	15.77–100	−0.35	0.40	0.55	0.91	0.31	0.35	0.38	0.95	0.38
ωB97XD	22.2–100	−0.21	0.31	0.43	0.93	0.31	0.32	0.36	0.96	0.32
M11	42.8–100	0.22	0.35	0.48	0.90	−0.24	0.28	0.33	0.97	0.32

[a] MSE denotes mean signed error in eV. MUE denotes mean unsigned error in eV. RMSE denotes root-mean-square error in eV. R^2 denotes the unitless square of the correlation coefficient from Fig. 3. [b] X denotes the percentage of nonlocal exchange.

performs worse than average will have a bar in the positive region. Eight functionals have all bars in the negative region; this includes the two global meta-GGAs (M05-2X and M06-2X) and six of the range-separated functionals, including M11. M11-L does extremely well as compared to all the other local functionals, with good performance for both valence and Rydberg excitations, but charge transfers are beyond the capability of local functionals. HSE is the worst range-separated functional, with performances below average for both valence and charge-transfer excitations, largely because of the lack of nonlocal exchange at LR. The CAM-B3LYP functional provides results that are better than HSE, but slightly worse than the other range-separated functionals, all of which have 100% nonlocal exchange at LR. As shown recently by Peach *et al.*[55] these performances might be eventually improved by considering variations of CAM-B3LYP that use 100% nonlocal exchange at LR.

4.2 The VT database

Statistical data on the results for the 103 S–S and the 63 S–T excitations of the VT database with the M11 and M11-L functionals are reported in Table 2 and compared to those of 15 other functionals from previous studies to results for the HSE functional calculated for the present work. Fig. 3 shows the correlation between the best estimates and the calculated results with M11 and M11-L.

It emerges that both M11 and M11-L perform very well for the whole VT set, in particular M11-L is the overall best performer among all considered functionals, with an overall MUE of 0.29 eV. M06-2X, M11, and ωB97X-D stand out as the other top functionals for the overall set.

Considering S–S and S–T excitations separately, it is already known,[7,20] that the percentage of nonlocal exchange plays a significant role for the description of the S–S excitations,

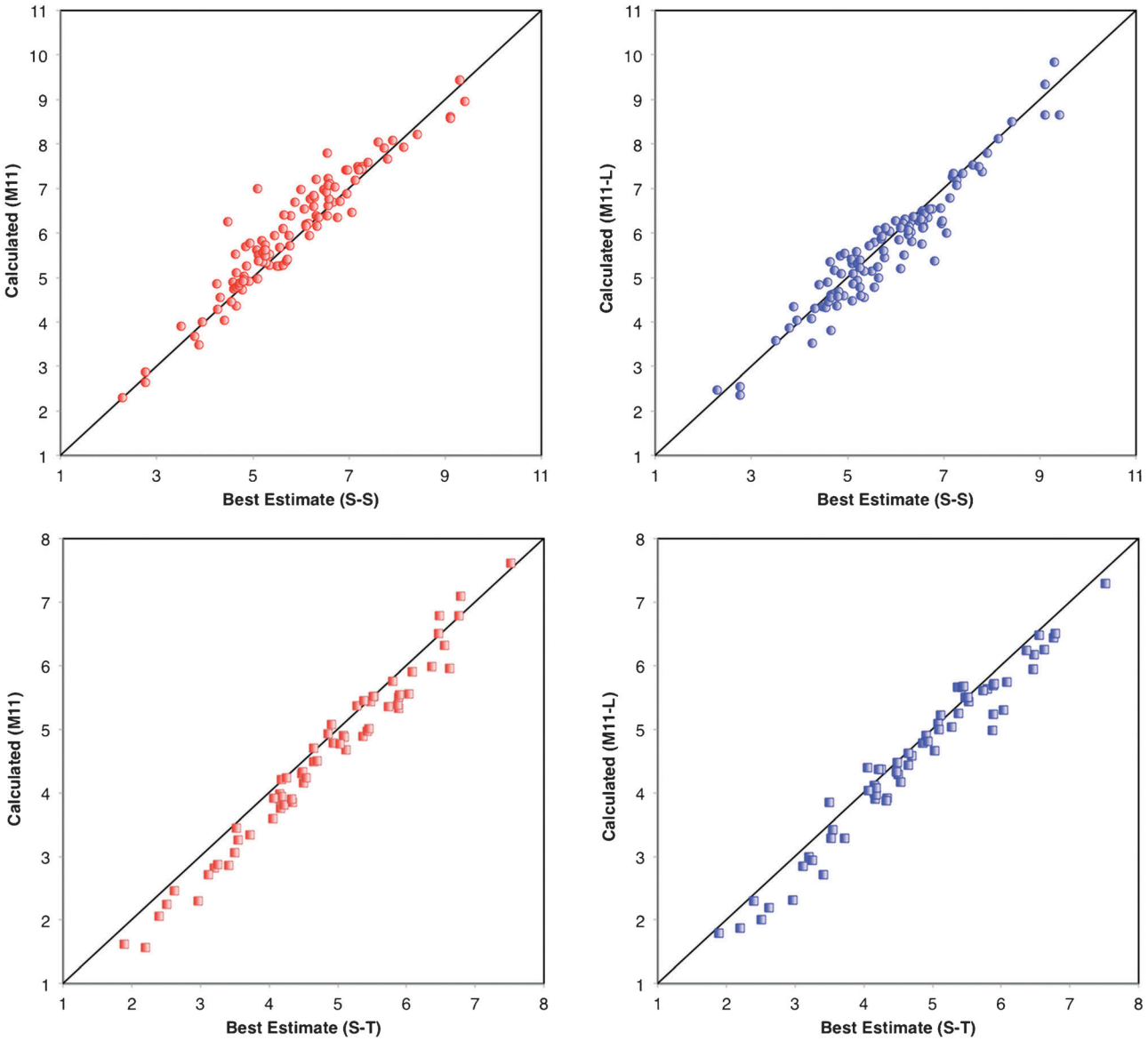

Fig. 3 Correlation plots for the VT set for singlet → singlet transitions (S–S, top, circles) and singlet → triplet transitions (S–T, bottom, squares), with M11 (left) and M11-L (right); all results are reported in eV.

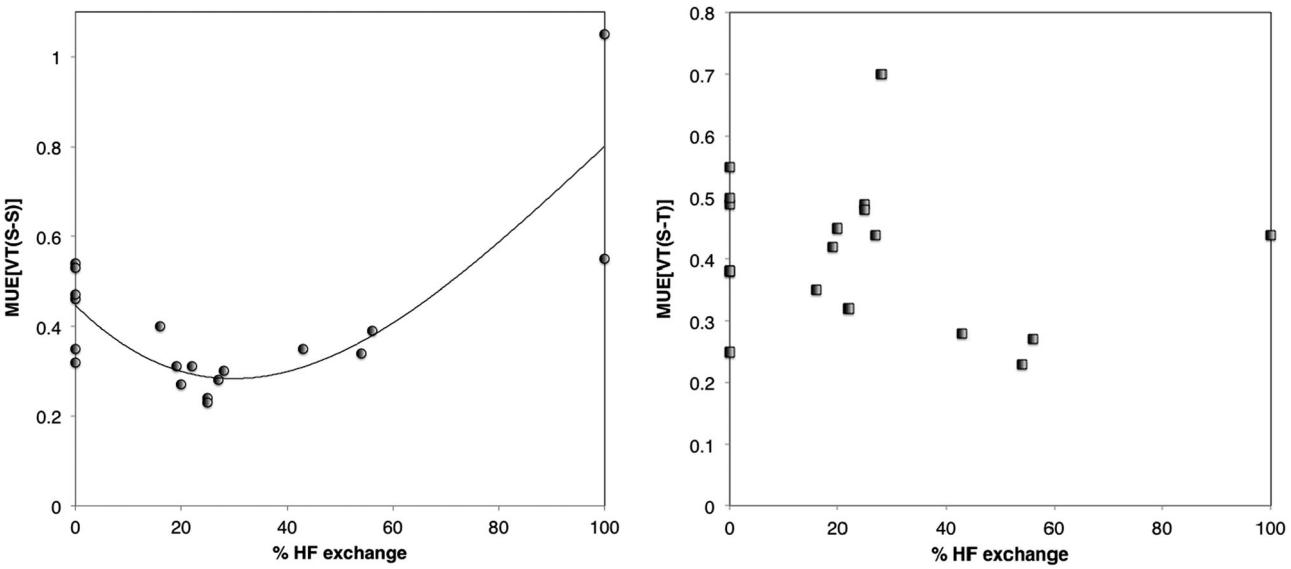

Fig. 4 Mean unsigned errors (MUEs, in eV) as a functions of the percentage of Hartree–Fock (HF) exchange for the VT set for singlet → singlet transitions (S–S, left, circles) and singlet → triplet transitions (S–T, right, squares). Range-separated hybrid functionals are classified according to the percentage of HF exchange at short-range. A parabolic trend line is added to the S–S plot, but no simple trend can be found for the S–T transitions.

but also that the functional form is crucial for the description of the S–T transitions. We found these trends in the plots of Fig. 4, where the performances of the functionals are plotted as a function of the percentage of nonlocal exchange. For the S–S transitions, functionals like PBE0, M05, and M06 with 25–28% nonlocal exchange are the top performers, a trend that is similar to that found for the VES20 database, which is not surprising since the VT set contains mainly valence excitations. Range-separated hybrids, including HSE and M11, follow this trend when the percentage of nonlocal exchange at short-range is considered (as in Fig. 4). As far as the S–T excitations, we note that such a clear trend as a function of the percentage of nonlocal exchange is no longer observed, and both our new functionals perform very accurately. M11-L is the best local functional in this category, outperforming the previous best functional M06-L by more than 34%. M11 is also the best performing functional among range-separated hybrids, being the only functional in its class to have an MUE below 0.30 eV. In general, the entire class of range-separated hybrids provide satisfactory results for these transitions, while among local and global hybrid functionals the performances are more diverse. In terms of overall MUE for the S–T transitions, M06-2X is the top performer, but both M11-L and M11 comes very close to it.

5 Conclusions

We find that in general, range-separated functionals perform much better than local functionals or global hybrids for TDDFT calculations of excited states. Among the range-separate hybrids, M11 has the best performance for charge-transfer states, and M11 performs better than any non-range-separated functional for Rydberg states, so it is a good choice for TDDFT. Other good choices include LC-ωPBE, ωB97, ωB97X, and M06-2X. Among these M11, ωB97X, and M06-2X are particularly appealing choices because of their known good behaviour for ground-state properties. Range-separated hybrid functionals, such as M11, are the best choice for a functional that needs to treat all three types of excitation energies.

The recently developed M11-L local functional is competitive with hybrid functionals for all excitations except charge transfer, (performance for the charge-transfer excitations remains, and will remain, a weak point of all local functionals), and therefore it is an excellent choice for extended systems, where local functionals have a major cost advantage. The success of M11-L is a further evidence that the dual-range exchange of M11-L is capable of a better compensation of the self-interaction error than any other previous local functional; see also, for example the much improved performances of M11-L for barrier heights[14] and for band gaps,[56] properties that are both very sensitive to the self-interaction error.

References

1 M. E. Casida, in *Recent Advances in Density Functional Methods, Part I*, ed. D. P. Chong, World Scientific, Singapore, 1995, pp. 155–192.
2 R. Bauernschmitt and R. Ahlrichs, *Chem. Phys. Lett.*, 1996, **256**, 454–464.
3 R. E. Stratmann, G. E. Scuseria and M. J. Frisch, *J. Chem. Phys.*, 1998, **109**, 8218–8224.
4 M. A. L. Marques and E. K. U. Gross, *Annu. Rev. Phys. Chem.*, 2004, **55**, 427–455.
5 D. Jacquemin, E. A. Perpéte, I. Ciofini, C. Adamo, R. Valero, Y. Zhao and D. G. Truhlar, *J. Chem. Theory Comput.*, 2010, **6**, 2071–2085.
6 J.-D. Chai and M. Head-Gordon, *J. Chem. Phys.*, 2008, **128**, 084106.
7 D. Jacquemin, E. A. Perpéte, I. Ciofini and C. Adamo, *Theor. Chem. Acc.*, 2010, **128**, 127–136.
8 R. Li, J. Zheng and D. G. Truhlar, *Phys. Chem. Chem. Phys.*, 2010, **12**, 12697–12701.
9 J. Plötner, D. J. Tozer and A. Dreuw, *J. Chem. Theory Comput.*, 2010, **6**, 2315–2324.

10 E. A. B. Kantchev, T. B. Norsten and M. B. Sullivan, *Proc. Comput. Sci.*, 2011, **4**, 1157–1166.
11 R. Peverati and D. G. Truhlar, *J. Phys. Chem. Lett.*, 2011, **2**, 2810–2817.
12 P. Gasiorski, K. S. Danel, M. Matusiewicz, T. Uchacz, W. Kuźnik, Ł. Piatek and A. V. Kityk, *Mater. Chem. Phys.*, 2012, **132**, 330–338.
13 D. Jacquemin, Y. Zhao, R. Valero, C. Adamo, I. Ciofini and D. G. Truhlar, *J. Chem. Theory Comput.*, 2012, **8**, 1255–1259.
14 R. Peverati and D. G. Truhlar, *J. Phys. Chem. Lett.*, 2012, **3**, 117–124.
15 T. Leininger, H. Stoll, H.-J. Werner and A. Savin, *Chem. Phys. Lett.*, 1997, **275**, 151–160.
16 H. Iikura, T. Tsuneda, T. Yanai and K. Hirao, *J. Chem. Phys.*, 2001, **115**, 3540–3544.
17 Y. Tawada, T. Tsuneda, S. Yanagisawa, T. Yanai and K. Hirao, *J. Chem. Phys.*, 2004, **120**, 8425.
18 D. Jacquemin, E. A. Perpéte, G. E. Scuseria, I. Ciofini and C. Adamo, *J. Chem. Theory Comput.*, 2008, **4**, 123–135.
19 J.-W. Song, M. A. Watson and K. Hirao, *J. Chem. Phys.*, 2009, **131**, 144108.
20 D. Jacquemin, E. A. Perpéte, I. Ciofini and C. Adamo, *J. Chem. Theory Comput.*, 2010, **6**, 1532–1537.
21 D. J. Tozer and N. C. Handy, *Phys. Chem. Chem. Phys.*, 2000, **2**, 2117–2121.
22 Y. Zhao and D. G. Truhlar, *Theor. Chem. Acc.*, 2008, **120**, 215–241.
23 M. J. G. Peach, P. Benfield, T. Helgaker and D. J. Tozer, *J. Chem. Phys.*, 2008, **128**, 044118.
24 Y. Zhao and D. G. Truhlar, *J. Phys. Chem. A*, 2006, **110**, 13126–13130.
25 Y. Zhao and D. G. Truhlar, *J. Chem. Theory Comput.*, 2008, **4**, 1849–1868.
26 K. Yang, R. Peverati, D. G. Truhlar and R. Valero, *J. Chem. Phys.*, 2011, **135**, 044118.
27 R. Send, M. Kühn and F. Furche, *J. Chem. Theory Comput.*, 2011, **7**, 2376–2386.
28 S. S. Leang, F. Zahariev and M. S. Gordon, *J. Chem. Phys.*, 2012, **136**, 104101.
29 T. Yanai, D. Tew and N. Handy, *Chem. Phys. Lett.*, 2004, **393**, 51–57.
30 J. Heyd, G. E. Scuseria and M. Ernzerhof, *J. Chem. Phys.*, 2003, **118**, 8207–8215.
31 Y. Zhao, R. Peverati, K. Yang and D. G. Truhlar, *MN-GFM, version 6.3: Minnesota Gaussian Functional Module*, University of Minnesota, Minneapolis, 2012.
32 M. J. Frisch, G. W. Trucks, H. B. Schlegel, G. E. Scuseria, M. A. Robb, J. R. Cheeseman, G. Scalmani, V. Barone, B. Mennucci, G. A. Petersson, H. Nakatsuji, M. Caricato, X. Li, H. P. Hratchian, A. F. Izmaylov, J. Bloino, G. Zheng, J. L. Sonnenberg, M. Hada, M. Ehara, K. Toyota, R. Fukuda, J. Hasegawa, M. Ishida, T. Nakajima, Y. Honda, O. Kitao, H. Nakai, T. Vreven, J. A. Montgomery, Jr., J. E. Peralta, F. Ogliaro, M. Bearpark, J. J. Heyd, E. Brothers, K. N. Kudin, V. N. Staroverov, R. Kobayashi, J. Normand, K. Raghavachari, A. Rendell, J. C. Burant, S. S. Iyengar, J. Tomasi, M. Cossi, N. Rega, J. M. Millam, M. Klene, J. E. Knox, J. B. Cross, V. Bakken, C. Adamo, J. Jaramillo, R. Gomperts, R. E. Stratmann, O. Yazyev, A. J. Austin, R. Cammi, C. Pomelli, J. Ochterski, R. L. Martin, K. Morokuma, V. G. Zakrzewski, G. A. Voth, P. Salvador, J. J. Dannenberg, S. Dapprich, A. D. Daniels, O. Farkas, J. B. Foresman, J. V. Ortiz, J. Cioslowski and D. J. Fox, *GAUSSIAN 09 (Revision A.1)*, Gaussian, Inc., Wallingford, CT, 2009.
33 A. Sadlej, *Theor. Chim. Acta*, 1991, **79**, 123–140.
34 M. E. Casida, C. Jamorski, K. C. Casida and D. R. Salahub, *J. Chem. Phys.*, 1998, **108**, 4439–4449.
35 A. Schafer, H. Horn and R. Ahlrichs, *J. Chem. Phys.*, 1992, **97**, 2571–2577.
36 A. Schafer, C. Huber and R. Ahlrichs, *J. Chem. Phys.*, 1993, **100**, 5829–5835.
37 A. D. Dwyer and D. J. Tozer, *Phys. Chem. Chem. Phys.*, 2010, **12**, 2816–2818.
38 M. Schreiber, M. R. Silva-Junior, S. P. A. Sauer and W. Thiel, *J. Chem. Phys.*, 2008, **128**, 134110.
39 M. R. Silva-Junior, M. Schreiber, S. P. A. Sauer and W. Thiel, *J. Chem. Phys.*, 2008, **129**, 104103.
40 S. P. A. Sauer, M. Schreiber, M. R. Silva-Junior and W. Thiel, *J. Chem. Theory Comput.*, 2009, **5**, 555–564.
41 A. V. Marenich, C. J. Cramer, D. G. Truhlar, C. A. Guido, B. Mennucci, G. Scalmani and M. J. Frisch, *Chem. Sci.*, 2011, **2**, 2143–2161.
42 M. R. Silva-Junior, S. P. A. Sauer, M. Schreiber and W. Thiel, *Mol. Phys.*, 2010, **108**, 453–465.
43 D. Jacquemin, V. Wathelet, E. A. Perpéte and C. Adamo, *J. Chem. Theory Comput.*, 2009, **5**, 2420–2435.
44 A. D. Becke, *Phys. Rev. A: At., Mol., Opt. Phys.*, 1988, **38**, 3098–3100.
45 C. Lee, W. Yang and R. G. Parr, *Phys. Rev. B*, 1987, **37**, 785–789.
46 J. P. Perdew, K. Burke and M. Ernzerhof, *Phys. Rev. Lett.*, 1996, **77**, 3865–3868.
47 Y. Zhao and D. G. Truhlar, *J. Chem. Phys.*, 2006, **125**, 194101.
48 A. D. Becke, *J. Chem. Phys.*, 1992, **98**, 5648–5652.
49 P. Stephens, F. Devlin, C. Chabalowski and M. J. Frisch, *J. Phys. Chem.*, 1993, **98**, 11623–11627.
50 J. P. Perdew, M. Ernzerhof and K. Burke, *J. Chem. Phys.*, 1996, **105**, 9982–9985.
51 Y. Zhao, N. E. Schultz and D. G. Truhlar, *J. Chem. Phys.*, 2005, **123**, 161103.
52 Y. Zhao, N. E. Schultz and D. G. Truhlar, *J. Chem. Theory Comput.*, 2005, **2**, 364–382.
53 O. A. Vydrov and G. E. Scuseria, *J. Chem. Phys.*, 2006, **125**, 234109.
54 J.-D. Chai and M. Head-Gordon, *Phys. Chem. Chem. Phys.*, 2008, **10**, 6615–6620.
55 M. J. G. Peach, T. Helgaker, P. Sałek, T. W. Keal, O. B. Lutnæs, D. J. Tozer and N. C. Handy, *Phys. Chem. Chem. Phys.*, 2006, **8**, 558–562.
56 R. Peverati and D. G. Truhlar, *J. Chem. Phys.*, 2012, **136**, 134704.

